

QTL Mapping in New *Arabidopsis thaliana* Advanced Intercross-Recombinant Inbred Lines

Sureshkumar Balasubramanian^{1,6,9}, Christopher Schwartz^{2,7,9}, Anandita Singh^{1,2a}, Norman Warthmann^{1,2}, Min Chul Kim^{1,2b}, Julin N. Maloof^{2,3}, Olivier Loudet^{2,5}, Gabriel T. Trainer², Tsegaye Dabi², Justin O. Borevitz^{2,4}, Joanne Chory^{2,8}, Detlef Weigel^{1,2*}

1 Department of Molecular Biology, Max Planck Institute for Developmental Biology, Tübingen, Germany, **2** Plant Biology Laboratory, The Salk Institute for Biological Sciences, La Jolla, California, United States of America, **3** Section of Plant Biology, University of California Davis, Davis, California, United States of America, **4** Department of Ecology and Evolution, University of Chicago, Chicago, Illinois, United States of America, **5** INRA, Genetics and plant breeding - SGAP, Versailles, France, **6** School of Biological Sciences, The University of Queensland, St. Lucia, Australia, **7** Department of Biochemistry, University of Wisconsin, Madison, Wisconsin, United States of America, **8** Howard Hughes Medical Institute, The Salk Institute for Biological Sciences, La Jolla, California, United States of America

Abstract

Background: Even when phenotypic differences are large between natural or domesticated strains, the underlying genetic basis is often complex, and causal genomic regions need to be identified by quantitative trait locus (QTL) mapping. Unfortunately, QTL positions typically have large confidence intervals, which can, for example, lead to one QTL being masked by another, when two closely linked loci are detected as a single QTL. One strategy to increase the power of precisely localizing small effect QTL, is the use of an intercross approach before inbreeding to produce Advanced Intercross RILs (AI-RILs).

Methodology/Principal Findings: We present two new AI-RIL populations of *Arabidopsis thaliana* genotyped with an average intermarker distance of 600 kb. The advanced intercrossing design led to expansion of the genetic map in the two populations, which contain recombination events corresponding to 50 kb/cM in an F₂ population. We used the AI-RILs to map QTL for light response and flowering time, and to identify segregation distortion in one of the AI-RIL populations due to a negative epistatic interaction between two genomic regions.

Conclusions/Significance: The two new AI-RIL populations, EstC and KendC, derived from crosses of Columbia (Col) to Estland (Est-1) and Kendallville (Kend-L) provide an excellent resource for high precision QTL mapping. Moreover, because they have been genotyped with over 100 common markers, they are also excellent material for comparative QTL mapping.

Citation: Balasubramanian S, Schwartz C, Singh A, Warthmann N, Kim MC, et al. (2009) QTL Mapping in New *Arabidopsis thaliana* Advanced Intercross-Recombinant Inbred Lines. PLoS ONE 4(2): e4318. doi:10.1371/journal.pone.0004318

Editor: Brian P. Dilkes, Purdue University, United States of America

Received: July 13, 2008; **Accepted:** December 22, 2008; **Published:** February 2, 2009

Copyright: © 2009 Balasubramanian et al. This is an open-access article distributed under the terms of the Creative Commons Attribution License, which permits unrestricted use, distribution, and reproduction in any medium, provided the original author and source are credited.

Funding: This work was supported by NIH NRSA Grant F23-GM65032-1 (CS), an EMBO Long-Term Fellowship ALTF-473 (SB), NIH grant GM62932 (JC & DW), ERA-PG (BMBF) Grant ARABRAS, and a Gottfried Wilhelm Leibniz Award from the DFG (DW), the Howard Hughes Medical Institute, and the Max Planck Society. The funders had no role in study design, data collection and analysis, decision to publish, or preparation of the manuscript.

Competing Interests: The authors have declared that no competing interests exist.

* E-mail: weigel@weigelworld.org

^{2a} Current address: TERI University, New Delhi, India

^{2b} Current address: Department of Agronomy, College of Agriculture and Life Science, Gyeongsang National University, Jinju, Korea

⁹ These authors contributed equally to this work.

Introduction

Deciphering the genetic basis of natural variation in quantitative traits presents a challenge because the variation is often continuous and because there is often extensive genotype × environment (G × E) interactions. An effective way towards identifying the causal sequence variants includes identification and molecular characterization of quantitative trait loci (QTL). Despite substantial progress in cloning QTL genes, and even reducing some of them to Quantitative Trait Nucleotides (QTNs), QTL mapping and cloning remain a formidable task [1–8]. One of the major impediments is that QTL mapping typically produces large genetic intervals, which make it difficult to determine the best candidates for the causal genes. In addition, QTL of large effect

can split into multiple QTL, with each explaining only a small proportion of the total variance.

An important factor influencing QTL confidence intervals is the number of recombination events in the mapping population. Therefore, if one increases the number of recombination events in each individual, precision improves without the need to phenotype a larger number of individuals. However, the success of this approach is dependent on how densely the population is genotyped, and requires a wealth of molecular polymorphism information across populations, which can then be exploited to develop markers for genotyping. Fortunately, in many species, mapping markers are no longer a rate-limiting factor. In the plant *Arabidopsis thaliana*, more than 300,000 non-singleton single nucleotide polymorphisms (SNPs) have recently been identified,

for an average density of two to three SNPs per kb [9]. This has further improved the value of *A. thaliana* for ecological and evolutionary genetics [10,11].

Recombinant Inbred Lines (RILs) are very useful in QTL analysis as they represent unique combinations of parental genotypes, and being immortal, they can be used for the analysis of many traits in many environments [12]. During the production of RILs, there are additional opportunities for recombination during the selfing generations, compared to simple F₂ populations. A further improvement is the advanced intercross approach, in which beginning with the F₁ or F₂ generation, individuals are randomly intercrossed, thus increasing the opportunity of recombination before genotypes are fixed upon selfing [13].

Several *A. thaliana* RIL populations have been used for QTL mapping and subsequent molecular identification of the responsible genes [14–30]. However, there are relatively few large populations that have been densely genotyped, limiting the resolution of QTL maps (Table S1). Here we describe two RIL populations generated using an advanced intercross (AI) design, which captures an increased number of recombination events. The map resolution of the AI-RIL populations, which have been genotyped with over 180 markers, is roughly equivalent to what one would expect in 800 F₂ individuals. We demonstrate the usefulness of the AI-RILs by mapping QTL for two traits, hypocotyl elongation and flowering time. In addition, we also identify two regions contributing to segregation distortion in one population.

Results and Discussion

RIL populations and genetic maps

The accessions Est-1 (Estland [Estonia]; CS6701) and Kend-L (Kendalville-Lehle; Lehle-WT-16-03) were crossed to the common lab strain Col (Columbia) as female. From the F₂ progeny, 75 non-overlapping pairs of plants were intercrossed for three generations to create advanced intercross lines. The resulting lines were taken through six rounds of selfing without any intentional selection (Figure 1). The resulting 279 EstC (Est-1×Col) lines and 282 KendC (Kend-L×Col) lines were genotyped at 224 and 181 markers, respectively (Tables S2, S3). The markers were drawn from a recently published set of SNPs that distinguish the Col-0 reference strains from many other accessions [31,32], as well as 45 SSLPs used for EstC (Table S2). There were 126 common markers for which Est-1 and Kend-L shared the same allele, which allows for combining mapping information across the two RIL populations. Genotyping was carried out using the MassARRAY platform [33].

The genetic maps for both AI-RIL populations were similar, with an average of nearly two markers per Mb and no gap between markers greater than 30 cM. Due to the advanced intercross design, the genetic distances were increased between markers compared to regular RILs, resulting in an expanded map with higher resolution (Figures 2A, B). The expansion of the two populations differed to some extent, which is revealed when the maps are compared directly using the 126 common markers (Figure 2C, D). The variation potentially reflects differences in recombination rates between the populations.

Segregation distortion

Many of the available *A. thaliana* RIL populations feature segregation distortion in selected regions of the genome [17,20,21,26,34]. Segregation distortion suggests either involuntary selection against these regions during generation of the RILs, or some type of incompatibility between genomic regions

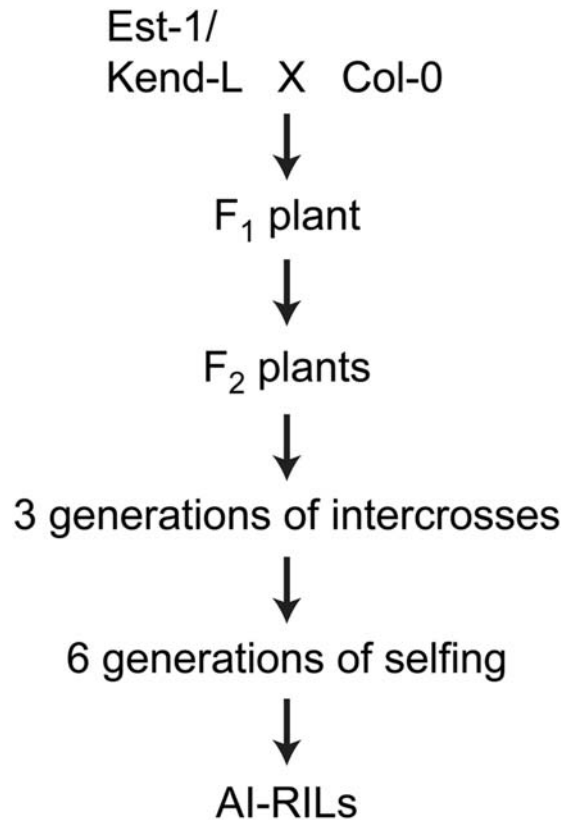


Figure 1. Diagram of the generation of AI-RILs. Intercrosses were between non-overlapping individuals.
doi:10.1371/journal.pone.0004318.g001

contributed by the different parents. For example, it has been reported that there are potential cases of reciprocal gene loss for paralogs located in segmental duplications, leading to some F₂ combinations lacking either functional copy [35].

While the KendC population did not show precise 50:50 segregation for all markers, there were no regions with strong deviation from this expectation. In contrast, we observed extreme segregation distortion in the EstC population. On chromosome 1, between 14 and 16 Mb, the Col alleles were substantially underrepresented, with only about one third of the expected frequency. The converse was found around 8.4 Mb on chromosome 5, where only 25% of the population is homozygous for the Est-1 allele (Figure 3A; Table 1). A chi-squared test suggested that distortion for the two regions was not independent (Figure 3B). Indeed, not a single AI-RIL was simultaneously homozygous for Col alleles in the chromosome 1 region and for Est-1 alleles in the chromosome 5 region.

To obtain additional information about the underlying cause of this interaction, we analyzed 500 F₂ plants at the most biased SSLP marker in each region (Table 2). While two markers on chromosome 4 segregated as expected (1:2:1 for homozygous and heterozygous classes, with an overall distribution of 1:1 for both alleles; data not shown), the alleles at chromosome 1 and 5 that were rare in the AI-RIL population were also rare in the F₂ population. In addition, none of the F₂ plants were Col homozygous at the chromosome 1 region and simultaneously homozygous for Est-1 at 8.4 Mb on chromosome 5. Therefore, the F₂ analysis recapitulated the EstC population results, indicating that the Col region at chromosome 1 is incompatible with an Est-1 region at chromosome 5. The F₂ experiment also demonstrates

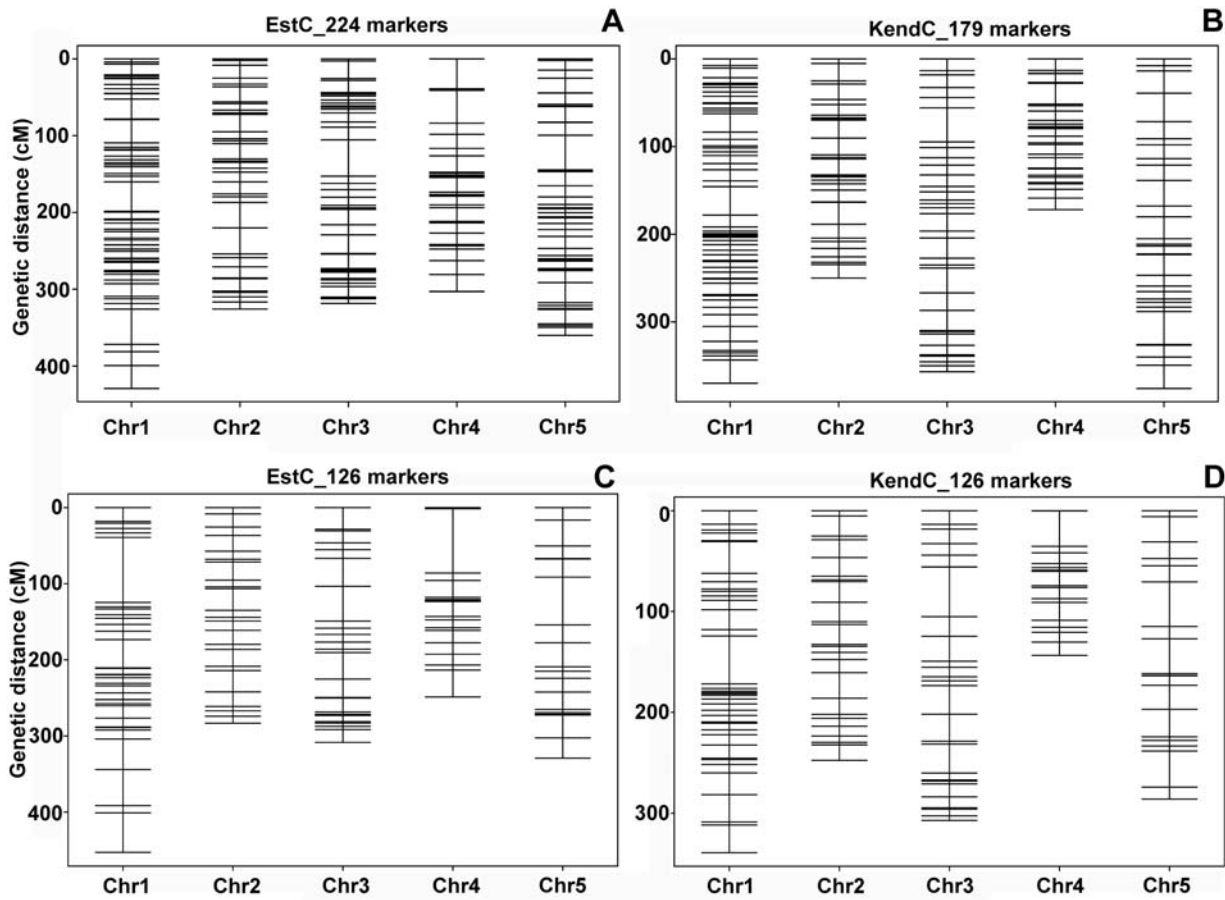


Figure 2. Genetic maps of AI-RIL populations. (A) Genetic map of EstC AI-RILs generated from the genotypes of 279 plants at 224 markers. (B) Genetic map of KendC AI-RILs generated using genotypes of 282 plants at 179 markers. (C, D) Genetic maps generated using the common 126 markers for the EstC (C) and KendC (D) populations. Note population-specific patterns of increases in genetic distances. doi:10.1371/journal.pone.0004318.g002

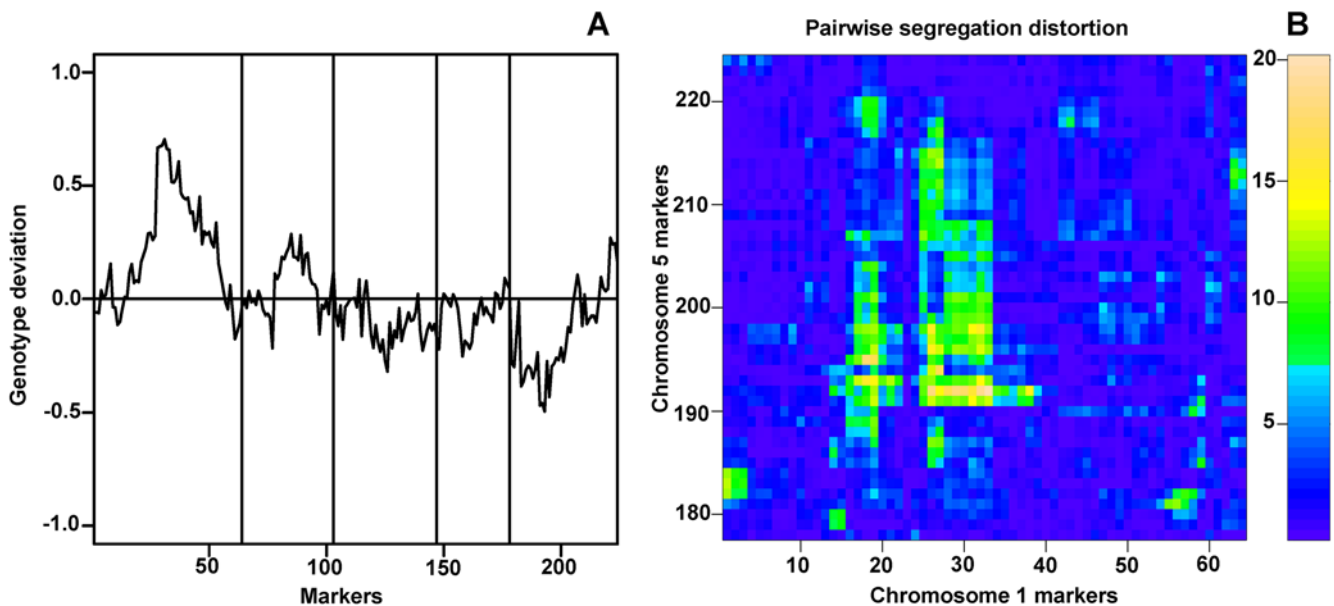


Figure 3. Segregation distortion in EstC AI-RILs. (A) Genotype of 224 markers over all five chromosomes. A value of 1.0 for a given marker represents all Est-1 alleles, while -1.0 corresponds to all Col alleles. (B) Chi-squared plot of pairwise segregation distortion for each marker on chromosome 1 and chromosome 5. Only the interaction between chromosome 1 and 5 markers are shown. Markers were consecutively numbered starting from the Northern most marker on chromosome 1. doi:10.1371/journal.pone.0004318.g003

Table 1. Distribution of genotypes at markers on chromosomes 1 and 5 in the EstC AI-RIL population.

Chromosome	Position (Mb)	Est allele	Col allele	Total
1	14.2	219	38	257
1	15.2	225	44	269
1	15.4	224	43	267
1	15.9	226	46	272
1	16	218	45	263
5	8.3	71	196	267
5	8.4	68	201	269
5	8.6	72	194	266

doi:10.1371/journal.pone.0004318.t001

that the missing genotypes must be eliminated at or before the seedling stage, since DNA for genotyping was isolated from young adult plants. The same two genomic regions also show segregation distortion in a number of other *A. thaliana* RIL populations, and the causative loci are being pursued (O. Loudet, unpublished results).

The mutually exclusive nature of the two regions makes epistatic analysis of loci involving these regions of the genomes problematic. Moreover, segregation distortion can affect marker order, as it creates spurious linkages. However, the availability of the genome sequence allowed us to fix the order of markers, which reduced the effects of segregation distortion on the genetic and QTL maps. Nevertheless, one needs to be aware that QTL located in these regions might not be properly identified.

Hypocotyl length QTL

To evaluate the power of the AI-RIL populations we assayed two traits under complex genetic control, hypocotyl length and flowering time, both of which are influenced by the light environment. Since hypocotyls were measured in seedlings, while flowering time was determined in adult plants, the comparison

Table 2. Chi-squared analysis of the genotypes in 422 F₂ plants derived from a cross between Est-1 and Col.

Genotypes		Observed (O)	Expected (E)	(O-E)	(O-E) ²	(O-E) ² /E
Chr_1	Chr_5					
Col	Col	32	26.4	5.6	31.7	1.2
Col	Est	0	26.4	-26.4	695.4	26.4
Col	Het	36	51.7	-15.7	246.5	4.8
Het	Col	43	51.7	-8.7	75.7	1.5
Het	Est	15	51.7	-36.7	1346.9	26.1
Het	Het	130	105.5	24.5	600.3	5.7
Est	Col	48	26.4	21.6	467.9	17.7
Est	Est	28	26.4	1.6	2.7	0.1
Est	Het	90	51.7	38.3	1466.9	28.4
					Chi-square sum	111.76*

* p < 0.0001

doi:10.1371/journal.pone.0004318.t002

between the two traits has the potential to provide information about light responsiveness at different developmental stages.

After seedlings germinate, they forage for light as an indicator of having broken the soil surface. Depending on the light environment, their embryonic stems, the hypocotyls, will be of different lengths. This trait is affected by both light quality and quantity, with seedlings grown in the dark having the longest hypocotyls. There is substantial variation in hypocotyl length among natural *A. thaliana* accessions, and several QTL for light-dependent hypocotyl length have been identified [36–38]. We analyzed the EstC population in four different light conditions (white, blue, red, far-red) and darkness. We found considerable variation in response to the four different light conditions along with transgression, suggesting that multiple loci contribute to variation in the EstC population (Figure 4; Table S2). Significant QTL, determined by permutation testing, were identified in all environments except darkness (Figure 5; Table S4). In white light, two QTL were significant, with a major-effect QTL detected on the top of chromosome 5 (Figure 5C), while in far-red light, a single marginally significant QTL was detected on the bottom of chromosome 4 (Figure 5D). In red light (Figure 5A), one QTL was identified on chromosome 1 (centered at 23.22 Mb), and a second one on chromosome 2 (centered at 8.20 Mb). The confidence interval for the second QTL in chromosome 2 included the *PHYB* locus (8.15 Mb). Est-1 has three polymorphisms compared to Col in the *PHYB* coding region, a 12 bp deletion near the initiation codon, and two nonsynonymous substitutions (I143L and L1072V). Among these, the I143L polymorphism has been recently to be associated with variation in red light response, making *PHYB* a good candidate for this QTL in the EstC population [39].

In blue light, one major QTL (*blue4*) was detected on the bottom of chromosome 4 (Figure 5B). We confirmed *blue4* both by repeating the phenotyping for a subset of AI-RILs (data not shown) and by exploiting heterogeneous inbred families (HIFs) derived from RIL 88, which is still heterozygous at the QTL (Figure 6A) [40]. QTL for hypocotyl length in this region, on the bottom of chromosome 4, have been previously identified in another RIL population in white, blue and red light conditions, suggesting that this region of the genome may harbor a QTL important for seedling light responsiveness [38]. However, given that the EstC QTL is detected only in blue light, it is possible that the causal gene in this case is different. Although several additional QTL peaks barely crossed the significance threshold on their own, a *scantwo* analysis (Figure 6B) revealed strong additive interactions for two regions (chromosomes 2 and 5) with the chromosome 4 QTL. Therefore, using HIFs derived from RIL 13, we tested and confirmed the interacting chromosome 5 QTL, demonstrating that this marginally significant QTL peak has significant phenotypic effects, and acts with *blue4* in an additive manner (Figure 6B).

Flowering time QTL

Flowering time, which is thought to be important for reproductive success in the wild, has been found to be highly variable among natural *A. thaliana* accessions [26,34,41–43]. We analyzed flowering time in the KendC population in both long days, which promote rapid flowering in many *A. thaliana* strains, and in short days (Table S3). Flowering time was measured using days to flowering (DTF) as well as the total number of leaves (TLN), partitioned into rosette and cauline leaves. QTL analysis (Figure 7A, B) identified a single strong QTL for both DTF and TLN in long days on the top of chromosome 5, with the Kend-L allele delaying flowering. A single marker association analysis

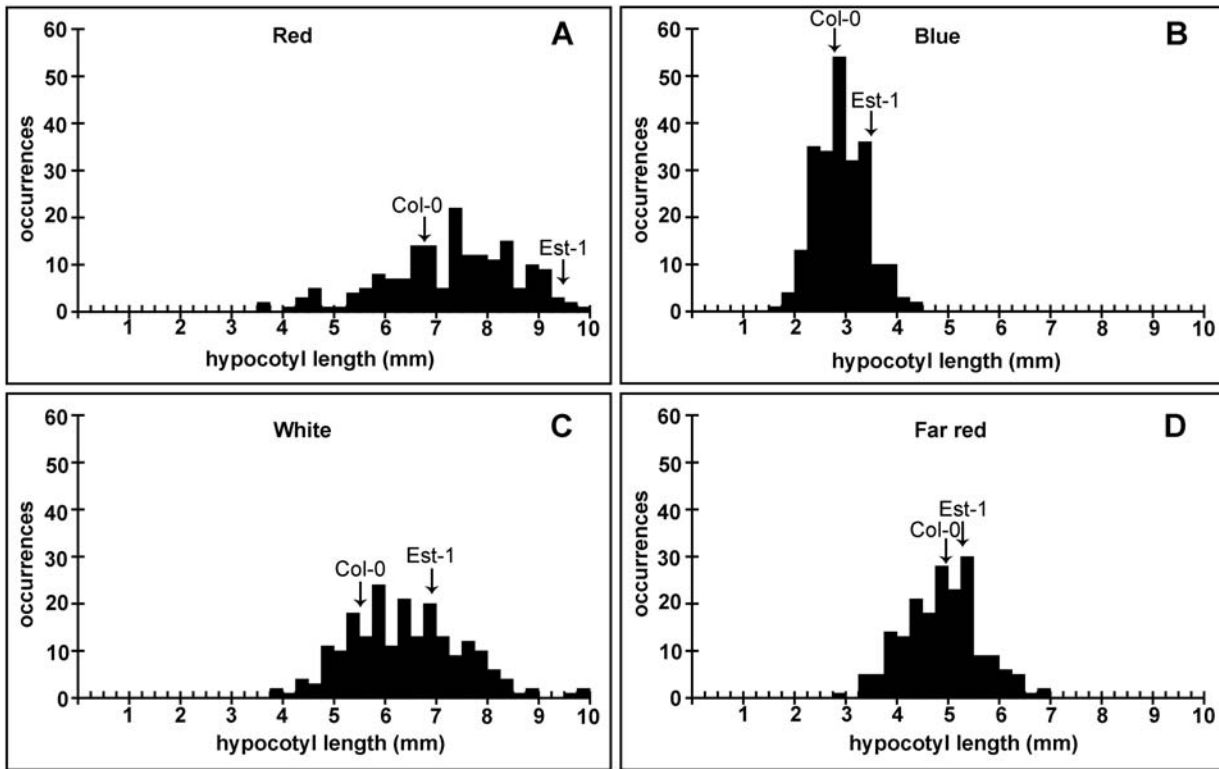


Figure 4. Variation in light response of EstC AI-RILs. Distributions of hypocotyl lengths under red (A), blue (B), white (C), and far-red (D) light are shown. doi:10.1371/journal.pone.0004318.g004

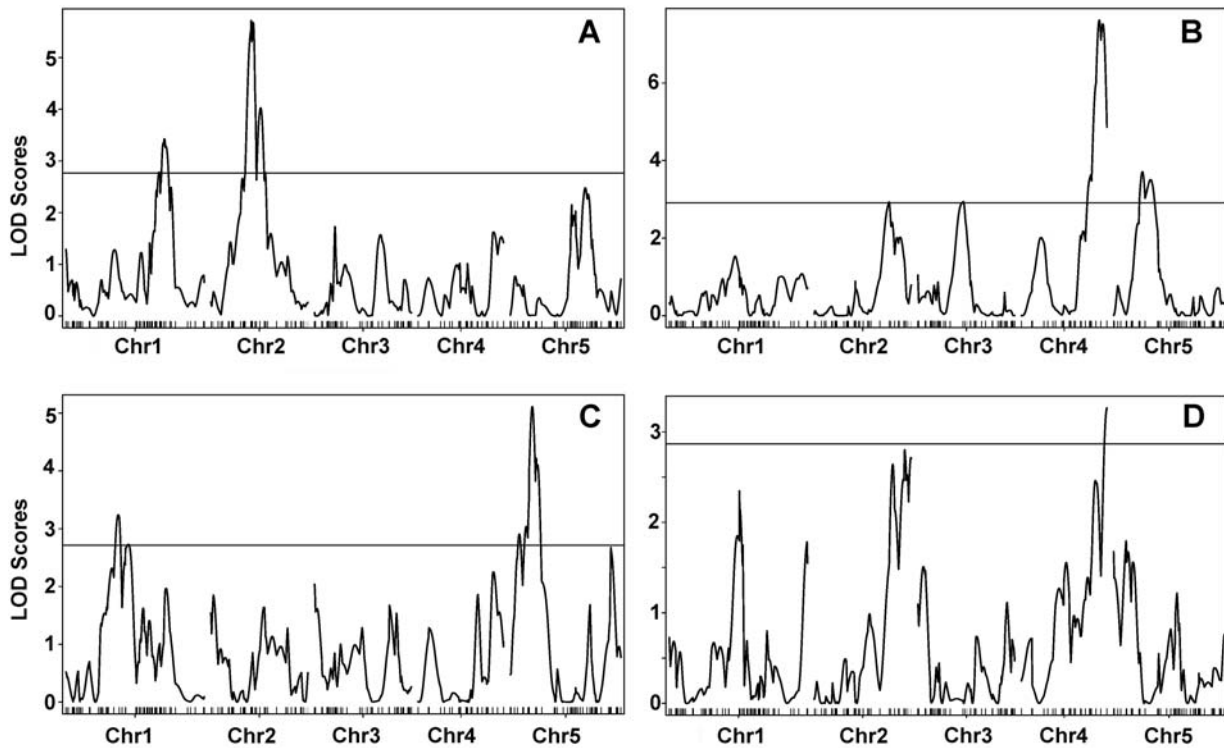


Figure 5. QTL analysis of hypocotyl elongation using EstC AI-RILs. QTL maps for red (A), blue (B), white (C), and far-red (D) are shown. Significant LOD scores were determined by permutation testing and are indicated by horizontal lines. doi:10.1371/journal.pone.0004318.g005

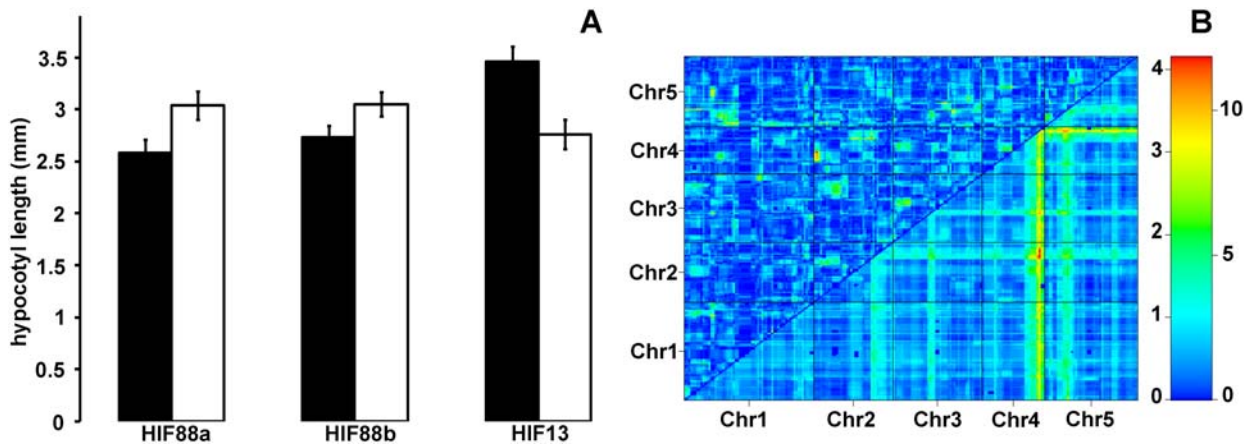


Figure 6. Confirmation of the chromosome 4 and 5 QTL for blue light response. (A) Comparison of hypocotyl lengths of heterogeneous inbred families segregating for the chromosome 4 (HIF88a and HIF88b) and 5 (HIF13) QTL. Col alleles are shown as black bars and Est-1 alleles as white bars. Error bars represent 95% confidence intervals. (B) A *scan-to-scan* analysis of blue light hypocotyl lengths. Top triangle shows epistasis, bottom shows additive interactions. Color scale indicates LOD scores for epistasis (left) and additive interactions (right). doi:10.1371/journal.pone.0004318.g006

revealed that the *Kend-L* alleles in the QTL region accounted for six to seven additional leaves in long days. This QTL encompasses a region that contains several flowering time genes. Foremost among them is *FLOWERING LOCUS C (FLC)*, a floral repressor that explains much of the natural variation in *A. thaliana* flowering [42–45]. Sequence analysis of the *Kend-L* allele of *FLC* revealed an insertion at the first intron of *FLC*. Intronic insertions at *FLC* typically lead to early flowering [42–45]. In this case, however, the Col allele confers early flowering, making *FLC* a less likely

candidate for the QTL. Further fine mapping is needed to confirm the causative gene(s) for the QTL.

A strong QTL for DTF was detected on top of chromosome 5 in short days as well (Figure 7C). While its position is similar to that of the chromosome 5 QTL observed in long days (Figure 7A,B), the markers with the strongest association for either QTL are two Mb apart, suggesting that different genes underlie each of these QTL. In contrast, the use of TLN as a proxy for flowering time identified a strong QTL on the bottom of

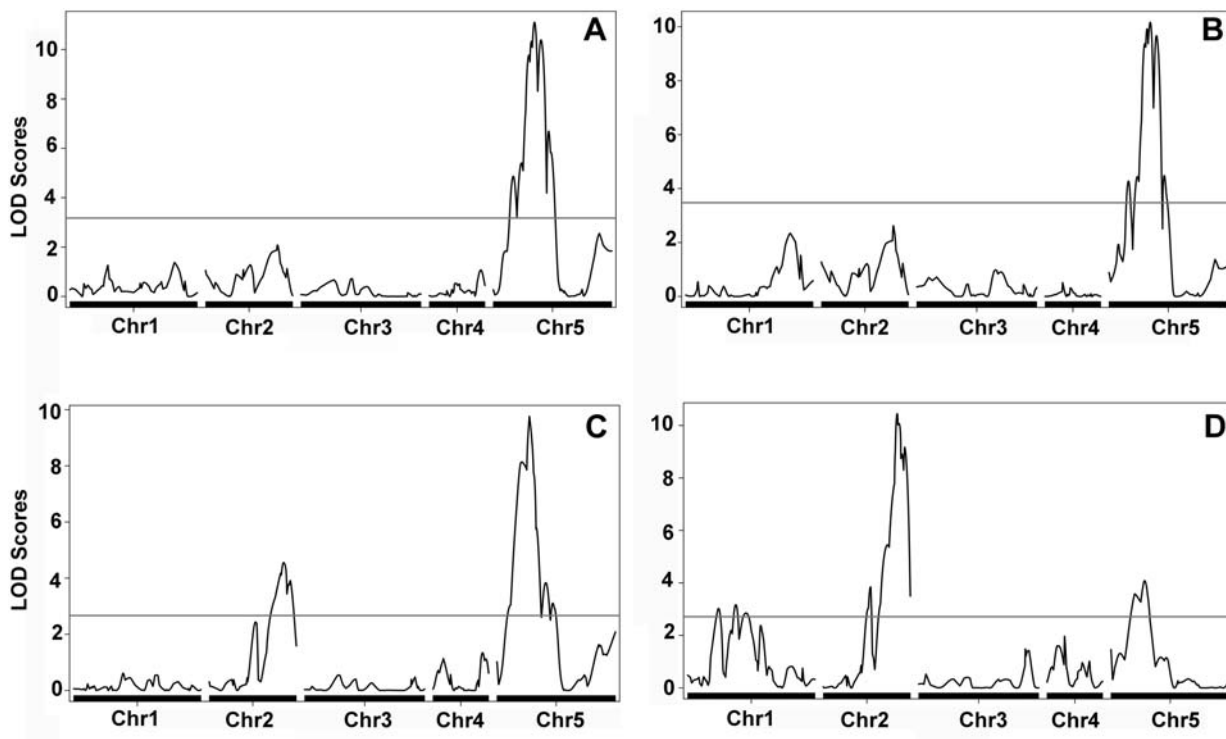


Figure 7. QTL analysis of flowering time in *KendC* AI-RILs. (A) QTL for days to flowering (DTF) in long days. (B) QTL for total leaf number (TLN) in long days. (C) QTL for DTF in short days. (D) QTL for TLN in short days. Note the magnitude of QTL effect changes with respect to the phenotype (DTF or TLN) in short days indicating a variation in growth. doi:10.1371/journal.pone.0004318.g007

chromosome 2, which was not found in long days (Figure 7B, D). In addition, the two QTLs detected in short days (chromosomes 2 and 5) differed in their magnitude, with the chromosome 5 locus being the major QTL for DTF (Figure 7C), and the chromosome 2 locus being the major QTL for TLN (Figure 7D). This difference in QTL underlying traits that are genetically correlated [42] indicates variation in developmental growth rate under short day conditions.

Conclusions

We have demonstrated the usefulness of the AI-RIL approach for *A. thaliana*. The two AI-RIL populations we describe, EstC and KendC, have been genotyped with well over a hundred markers, most of which are in common for both populations. Due to the large number of fixed recombination events, the size of the AI-RIL sets, and the density of markers, these populations provide an excellent resource for QTL analysis (Table S4).

Materials and Methods

Plant material

The RIL parents Est-1 (Estland; CS6701; male) and Kend-L (Kendalville, MI USA; Lehle-WT-16-03; male) were obtained from the ABRC (Arabidopsis Biological Resource Center, Ohio State University, OH, USA) and from Lehle Seeds (Round Rock, TX, USA), respectively. The final AI-RIL populations have been submitted to the *Arabidopsis* stock center and are available under stock numbers CS39389 (EstC) and CS39697 (KendC).

Hypocotyl length analysis

Seeds were sterilized in 1.5-ml microcentrifuge tubes for 10 min in 70% ethanol, 0.01% Triton X-100, washed in 95% ethanol, and resuspended in sterile water. 60–70 seeds for each RIL were imbibed overnight and spotted individually on plates containing ½ Murashige and Skoog salts, 0.7% Phytagar with sufficient space to avoid seedling shading. Plates were placed at 4°C in the dark for 3 days, exposed to white light ($120 \mu\text{E m}^{-2} \text{sec}^{-1}$) for 4 hours to induce germination (with the exception of plates destined for far-red conditions, where exposure to white light was increased to 12 hours to overcome any far-red induced inhibition of germination), and placed under the appropriate condition. Blue, red and far-red light treatments were conducted in Percival E30LED chambers (Percival Scientific, Boone, IA USA), while white light and dark treatments were carried out in a Percival E30B chamber with the dark sample wrapped in aluminum foil. Seeds were grown in white ($40 \mu\text{E m}^{-2} \text{sec}^{-1}$), blue ($4.2 \mu\text{E m}^{-2} \text{sec}^{-1}$), red ($35 \mu\text{E m}^{-2} \text{sec}^{-1}$), or far-red ($0.5 \mu\text{E m}^{-2} \text{sec}^{-1}$) light and the dark at 22°C for 7 days. Fluence rate was determined by using a Li-Cor1800 spectroradiometer (Li-Cor Biosciences, Lincoln, NE USA).

Analyses in all five conditions were done in the same week to minimize week-to-week variation of growth conditions and seed quality. Germination was recorded in white light conditions, in 12 hour intervals. The germination scores (0–3) were treated as a phenotype. QTL mapping with this phenotype did not reveal any significant QTL affecting this trait (data not shown).

HIF lines, derived from RIL88 (a = S6 and b = S7) and RIL13 (S7), were grown in blue light to confirm QTL for the blue light response on chromosomes 4 and 5. Fifty to 80 seedlings were measured for each homozygous genotype. In addition, the chromosome 4 QTL was confirmed with a random subset of 80

EstC AI-RILs under a lower fluence of blue light ($3.0 \mu\text{E m}^{-2} \text{sec}^{-1}$; data not shown).

In total, over 16,000 seedlings were transferred to an acetate sheet covered with a moist paper towel and scanned on a flatbed scanner. Hypocotyl lengths were measured using NIH Image 1.62 (National Institutes of Health).

Flowering time analysis

For the KendC population, 12 plants per RIL line were planted in a completely randomized design as previously described [42,46] in both long-days and short days at 23°C. The growth conditions and the methodology of flowering time measurements have been described [42,46].

QTL mapping and statistical analyses

The KendC population was genotyped with 181 SNP markers. The EstC population was genotyped with 45 established SSLP markers [21,47] and 179 SNP markers [32]. Genetic linkage maps were determined using Joinmap 3 [48]; the marker orders agreed with the published Col-0 sequence. QTL analysis was carried out with the R-qtl package (<http://www.rqtl.org>) implemented in R (<http://www.r-project.org>), via interval mapping using the EM algorithm [49]. LOD thresholds established using one thousand permutations were used to determine the significance of the QTLs. The bQTL package (<http://famprevmed.ucsd.edu:16080/faculty/cberry/bqtl/>) in R was used to perform a chi-squared test for marker association (segregation distortion). All other statistical analysis was carried out using JMP (<http://www.jmp.com>). A summary of the identified QTL is given in Table S4.

Supporting Information

Table S1 Comparisons of publicly available RIL populations with the the EstC and KendC AI-RIL populations.

Found at: doi:10.1371/journal.pone.0004318.s001 (0.03 MB XLS)

Table S2 Genotype information and hypocotyl length data for EstC AI-RILs.

Found at: doi:10.1371/journal.pone.0004318.s002 (1.79 MB XLS)

Table S3 Genotype information and flowering time data for KendC AI-RILs.

Found at: doi:10.1371/journal.pone.0004318.s003 (0.77 MB XLS)

Table S4 Summary of QTL identified.

Found at: doi:10.1371/journal.pone.0004318.s004 (0.01 MB XLS)

Acknowledgments

We thank the NSF-funded Arabidopsis Biological Resource Center and Lehle Seeds for seeds, and Josip Perkovic and Ashley Goodman for help with plant work.

Author Contributions

Conceived and designed the experiments: SB CS JM JOB JC DW. Performed the experiments: SB CS AS MCK JM OL GTT TD JOB. Analyzed the data: SB CS NW JM JOB. Wrote the paper: SB CS JM JOB JC DW. Coordinated research: DW JC. Generated RILs: SB CS AS MCK JM GTT TD JOB. Phenotyped RILs: SB CS AS MCK JM OL JOB.

References

1. Ron M, Weller JI (2007) From QTL to QTN identification in livestock—winning by points rather than knock-out: a review. *Anim Genet* 38: 429–439.
2. Holland JB (2007) Genetic architecture of complex traits in plants. *Curr Opin Plant Biol* 10: 156–161.
3. Salvi S, Tuberosa R (2005) To clone or not to clone plant QTLs: present and future challenges. *Trends Plant Sci* 10: 297–304.
4. Darvasi A (2005) Dissecting complex traits: the geneticists’ “Around the world in 80 days”. *Trends Genet* 21: 373–376.
5. Borevitz JO, Chory J (2004) Genomics tools for QTL analysis and gene discovery. *Curr Opin Plant Biol* 7: 132–136.
6. Rikke BA, Johnson TE (1998) Towards the cloning of genes underlying murine QTLs. *Mamm Genome* 9: 963–968.
7. Weigel D, Nordborg M (2005) Natural variation in *Arabidopsis*. How do we find the causal genes? *Plant Physiol* 138: 567–568.
8. Wu R, Lin M (2006) Functional mapping - how to map and study the genetic architecture of dynamic complex traits. *Nat Rev Genet* 7: 229–237.
9. Clark RM, Schweikert G, Toomajian C, Ossowski S, Zeller G, et al. (2007) Common sequence polymorphisms shaping genetic diversity in *Arabidopsis thaliana*. *Science* 317: 338–342.
10. Mitchell-Olds T, Schmitt J (2006) Genetic mechanisms and evolutionary significance of natural variation in *Arabidopsis*. *Nature* 441: 947–952.
11. Shindo C, Bernasconi G, Hardtke CS (2007) Natural genetic variation in *Arabidopsis*: tools, traits and prospects for evolutionary ecology. *Ann Bot* 99: 1043–1054.
12. Burr B, Burr FA (1991) Recombinant inbreds for molecular mapping in maize: theoretical and practical considerations. *Trends Genet* 7: 55–60.
13. Darvasi A, Soller M (1995) Advanced intercross lines, an experimental population for fine genetic mapping. *Genetics* 141: 1199–1207.
14. Clerckx EJ, El-Lithy ME, Vierling E, Ruys GJ, Blankestijn-De Vries H, et al. (2004) Analysis of natural allelic variation of *Arabidopsis* seed germination and seed longevity traits between the accessions Landsberg *erecta* and Shakhara, using a new recombinant inbred line population. *Plant Physiol* 135: 432–443.
15. O’Neill CM, Morgan C, Kirby J, Tschopp H, Deng PX, et al. (2008) Six new recombinant inbred populations for the study of quantitative traits in *Arabidopsis thaliana*. *Theor Appl Genet* 116: 623–634.
16. el-Lithy ME, Bentsink L, Hanhart CJ, Ruys GJ, Rovito D, et al. (2006) New *Arabidopsis* recombinant inbred line populations genotyped using SNPWave and their use for mapping flowering-time quantitative trait loci. *Genetics* 172: 1867–1876.
17. Alonso-Blanco C, Peeters AJ, Koornneef M, Lister C, Dean C, et al. (1998) Development of an AFLP based linkage map of *Ler*, *Col* and *Cvi* *Arabidopsis thaliana* ecotypes and construction of a *Ler*/*Cvi* recombinant inbred line population. *Plant J* 14: 259–271.
18. Lister C, Dean C (1993) Recombinant inbred lines for mapping RFLP and phenotypic markers in *A. thaliana*. *Plant J* 4: 745–750.
19. Wilson IW, Schiff CL, Hughes DE, Somerville SC (2001) Quantitative trait loci analysis of powdery mildew disease resistance in the *Arabidopsis thaliana* accession Kashmir-1. *Genetics* 158: 1301–1309.
20. Torjek O, Witucka-Wall H, Meyer RC, von Korff M, Kusterer B, et al. (2006) Segregation distortion in *Arabidopsis* C24/*Col-0* and *Col-0*/*C24* recombinant inbred line populations is due to reduced fertility caused by epistatic interaction of two loci. *Theor Appl Genet* 113: 1551–1561.
21. Loudet O, Chaillou S, Camilleri C, Bouchez D, Daniel-Vedele F (2002) Bay-0xShahdara recombinant inbred line population: a powerful tool for the genetic dissection of complex traits in *Arabidopsis*. *Theor Appl Genet* 104: 1173–1184.
22. Magliano TM, Botto JF, Godoy AV, Symonds VV, Lloyd AM, et al. (2005) New *Arabidopsis* recombinant inbred lines (Landsberg *erecta*xNossen) reveal natural variation in phytochrome-mediated responses. *Plant Physiol* 138: 1126–1135.
23. Keurentjes JJ, Bentsink L, Alonso-Blanco C, Hanhart CJ, Blankestijn-De Vries H, et al. (2007) Development of a near-isogenic line population of *Arabidopsis thaliana* and comparison of mapping power with a recombinant inbred line population. *Genetics* 175: 891–905.
24. Simon M, Loudet O, Durand S, Berard A, Brunel D, et al. (2008) Quantitative trait loci mapping in five new large recombinant inbred line populations of *Arabidopsis thaliana* genotyped with consensus single-nucleotide polymorphism markers. *Genetics* 178: 2253–2264.
25. El-Assal SE-D, Alonso-Blanco C, Peeters AJ, Raz V, Koornneef M (2001) A QTL for flowering time in *Arabidopsis* reveals a novel allele of *CRT2*. *Nat Genet* 29: 435–440.
26. Werner JD, Borevitz JO, Warthmann N, Trainer GT, Ecker JR, et al. (2005) Quantitative trait locus mapping and DNA array hybridization identify an *FLM* deletion as a cause for natural flowering-time variation. *Proc Natl Acad Sci U S A* 102: 2460–2465.
27. Loudet O, Saliba-Colombani V, Camilleri C, Calenge F, Gaudon V, et al. (2007) Natural variation for sulfate content in *Arabidopsis thaliana* is highly controlled by *APR2*. *Nat Genet* 39: 896–900.
28. Svistoonoff S, Creff A, Reymond M, Sigoillot-Claude C, Ricaud L, et al. (2007) Root tip contact with low-phosphate media reprograms plant root architecture. *Nat Genet* 39: 792–796.
29. Deslandes L, Pileur F, Liaubet L, Camut S, Can C, et al. (1998) Genetic characterization of *RRS1*, a recessive locus in *Arabidopsis thaliana* that confers resistance to the bacterial soilborne pathogen *Ralstonia solanacearum*. *Mol Plant Microbe Interact* 11: 659–667.
30. Zhang Z, Ober JA, Kliebenstein DJ (2006) The gene controlling the quantitative trait locus *EPITHIOSPECIFIER MODIFIER1* alters glucosinolate hydrolysis and insect resistance in *Arabidopsis*. *Plant Cell* 18: 1524–1536.
31. Nordborg M, Hu TT, Ishino Y, Jhaveri J, Toomajian C, et al. (2005) The pattern of polymorphism in *Arabidopsis thaliana*. *PLoS Biol* 3: e196.
32. Warthmann N, Fitz J, Weigel D (2007) MSQT for choosing SNP assays from multiple DNA alignments. *Bioinformatics* 23: 2784–2787.
33. Jurinke C, van den Boom D, Cantor CR, Koster H (2001) Automated genotyping using the DNA MassArray technology. *Methods Mol Biol* 170: 103–116.
34. Alonso-Blanco C, El-Assal SE, Coupland G, Koornneef M (1998) Analysis of natural allelic variation at flowering time loci in the Landsberg *erecta* and Cape Verde Islands ecotypes of *Arabidopsis thaliana*. *Genetics* 149: 749–764.
35. Staal J, Kaliff M, Bohman S, Dixelius C (2006) Transgressive segregation reveals two *Arabidopsis* TIR-NB-LRR resistance genes effective against *Leptosphaeria maculans*, causal agent of blackleg disease. *Plant J* 46: 218–230.
36. Borevitz JO, Maloof JN, Lutes J, Dabi T, Redfern JL, et al. (2002) Quantitative trait loci controlling light and hormone response in two accessions of *Arabidopsis thaliana*. *Genetics* 160: 683–696.
37. Maloof JN, Borevitz JO, Dabi T, Lutes J, Nehring RB, et al. (2001) Natural variation in light sensitivity of *Arabidopsis*. *Nat Genet* 29: 441–446.
38. Wolyn DJ, Borevitz JO, Loudet O, Schwartz C, Maloof J, et al. (2004) Light-response quantitative trait loci identified with composite interval and eXtreme array mapping in *Arabidopsis thaliana*. *Genetics* 167: 907–917.
39. Filiault DL, Wessinger CA, Dinneny JR, Lutes J, Borevitz JO, et al. (2008) Amino acid polymorphisms in *Arabidopsis* phytochrome B cause differential responses to light. *Proc Natl Acad Sci U S A* 105: 3157–3162.
40. Tuinstra M, Ejeta G, Goldsbrough P (1997) Heterogenous inbred family (HIF) analysis: a method for developing near-isogenic lines that differ at quantitative trait loci. *Theor Appl Genet* 95: 1005–1011.
41. Stinchcombe JR, Weinig C, Ungerer M, Olsen KM, Mays C, et al. (2004) A latitudinal cline in flowering time in *Arabidopsis thaliana* modulated by the flowering time gene *FRIGIDA*. *Proc Natl Acad Sci U S A* 101: 4712–4717.
42. Lempe J, Balasubramanian S, Sureshkumar S, Singh A, Schmid M, et al. (2005) Diversity of flowering responses in wild *Arabidopsis thaliana* strains. *PLoS Genet* 1: 109–118.
43. Shindo C, Aranzana MJ, Lister C, Baxter C, Nicholls C, et al. (2005) Role of *FRIGIDA* and *FLOWERING LOCUS C* in determining variation in flowering time of *Arabidopsis*. *Plant Physiol* 138: 1163–1173.
44. Gazzani S, Gendall AR, Lister C, Dean C (2003) Analysis of the molecular basis of flowering time variation in *Arabidopsis* accessions. *Plant Physiol* 132: 1107–1114.
45. Shindo C, Lister C, Crevillen P, Nordborg M, Dean C (2006) Variation in the epigenetic silencing of *FLC* contributes to natural variation in *Arabidopsis* vernalization response. *Genes Dev* 20: 3079–3083.
46. Balasubramanian S, Sureshkumar S, Lempe J, Weigel D (2006) Potent induction of *Arabidopsis thaliana* flowering by elevated growth temperature. *PLoS Genet* 2: e106.
47. Bell CJ, Ecker JR (1994) Assignment of 30 microsatellite loci to the linkage map of *Arabidopsis*. *Genomics* 19: 137–144.
48. Stam P (1993) Construction of integrated genetic linkage maps by means of a new computer package: JOINMAP. *The Plant Journal* 3: 739–744.
49. Broman KW, Wu H, Sen S, Churchill GA (2003) R/qtl: QTL mapping in experimental crosses. *Bioinformatics* 19: 889–890.